

## Supporting Information

### Switching to “Turn-on” Fluorescent Probe for Selective Monitoring Cyanide in Food Samples and Living Systems

Hai Wu,<sup>\*a,b</sup> Miaomiao Chen,<sup>a,b</sup> Qinqin Xu,<sup>a</sup> Ying Zhang,<sup>a</sup> Pingping Liu,<sup>a</sup> Wenyong Li,<sup>\*b</sup>  
and Suhua Fan<sup>\*a</sup>

<sup>a</sup>School of Chemistry and Materials Engineering, Fuyang Normal University, Fuyang,  
Anhui 236037, PR China.

<sup>b</sup>Anhui Province Key Laboratory of Environmental Hormone and Reproduction,  
Anhui Province Key Laboratory for Degradation and Monitoring of Pollution of the  
Environment, Fuyang Normal University, Fuyang, Anhui 236037, PR China.

\* Corresponding authors. Tel.: +86 558 2596249; Fax: +86 558 2596249.

*E-mail addresses:* wuhai317@163.com; liwenyong@aliyun.com;  
fansuhua@fudan.edu.cn

## 1. Materials

All chemical reagents including reagents, anions and solvents used in synthesis, and characterization were purchased from Energy Chemical (Shanghai, China) and Aladdin (Shanghai, China) and used without further purification. Aqueous solutions in this article were prepared with high-purity water.

## 2. Synthesis and Characterizations of TPA-MT and TPA-BTD-MT.

The synthetic routes and characterizations for TPA-MT and TPA-BTD-MT are shown in **Scheme S1** and **Fig. S14-S18**.

### 2.1. Synthesis of 4-(7-bromobenzo[c][1,2,5]thiadiazol-4-yl)-N, N- diphenylaniline (TPA-BTD-Br)

Under a nitrogen atmosphere, a degassed mixture of toluene (50 mL), THF (50 mL), and water (20 mL) was added to a flask charged with 4,7-dibromobenzo[c][1,2,5]thiadiazole (1.46 g, 5 mmol), 4-(diphenylamino)phenylboronic acid (1.73 g, 6 mmol), Pd(PPh<sub>3</sub>)<sub>4</sub> (88.5 mg, 0.077 mmol) and K<sub>2</sub>CO<sub>3</sub> (1.13 g, 8.19 mol). The resulting mixture was stirred at 85 °C for 16 h. The solution was extracted with dichloromethane twice. Then, the organic solution was dried by anhydrous sodium sulfate. The crude compound was column purified using petroleum ether/DCM (v/v=3.5:1) to obtain the desired product compound (1.14 g, 50% yield). <sup>1</sup>H NMR (CDCl<sub>3</sub>, 400 MHz, δ/ppm): 7.82 (d, *J* = 7.60 Hz, 1H), 7.73 (d, *J* = 8.76 Hz, 2H), 7.49 (d, *J* = 7.64 Hz, 1H), 7.18-7.24 (m, 5H), 7.10-7.12 (m, 5H), 6.98-7.02 (m, 2H). <sup>13</sup>C NMR (CDCl<sub>3</sub>, 100 MHz, δ/ppm): 152.95, 152.13, 147.42, 146.31, 132.55, 131.34, 128.87, 128.81, 128.37, 126.29, 124.01, 122.49, 121.59, 111.16.

## 2.2. Synthesis of 4-(7-(4-(diphenylamino)phenyl)benzo[c][1,2,5]thiadiazol-4-yl)benzaldehyde (TPA-BTD-CHO)

A mixture of TPA-BTD-Br (1.37 g, 3.0 mol), 4-formylphenylboronic acid (675 mg, 4.5 mmol), Pd(PPh<sub>3</sub>)<sub>4</sub> (52 mg, 0.045 mmol) and K<sub>2</sub>CO<sub>3</sub> (669 mg, 4.85 mol) was added to toluene (40 mL), THF (60 mL), and water (20 mL) under a nitrogen atmosphere. The reaction mixture was stirred at 85 °C for 16 h and then poured into 100 mL water. The mixture was extracted with dichloromethane for twice. The combined organic solution was dried by anhydrous sodium sulfate. Then the concentrated solution was purified by column chromatography using DCM as an eluent to obtain an orange solid (50% yield). <sup>1</sup>H NMR (CDCl<sub>3</sub>, 400 MHz, δ/ppm): 10.03 (s, 1H), 7.92 (d, *J* = 8.16 Hz, 2H), 7.72 (d, *J* = 8.12 Hz, 2H), 7.52 (d, *J* = 8.60 Hz, 2H), 7.26-7.31 (m, 5H), 7.05-7.15 (m, 9H). <sup>13</sup>C NMR (CDCl<sub>3</sub>, 100 MHz, δ/ppm): 191.90, 148.45, 147.36, 146.65, 134.70, 132.80, 130.35, 129.42, 128.04, 126.91, 124.90, 123.50, 123.13.

## 2.3. Synthesis of 4'-(diphenylamino)biphenyl-4-carbaldehyde (TPA-CHO)

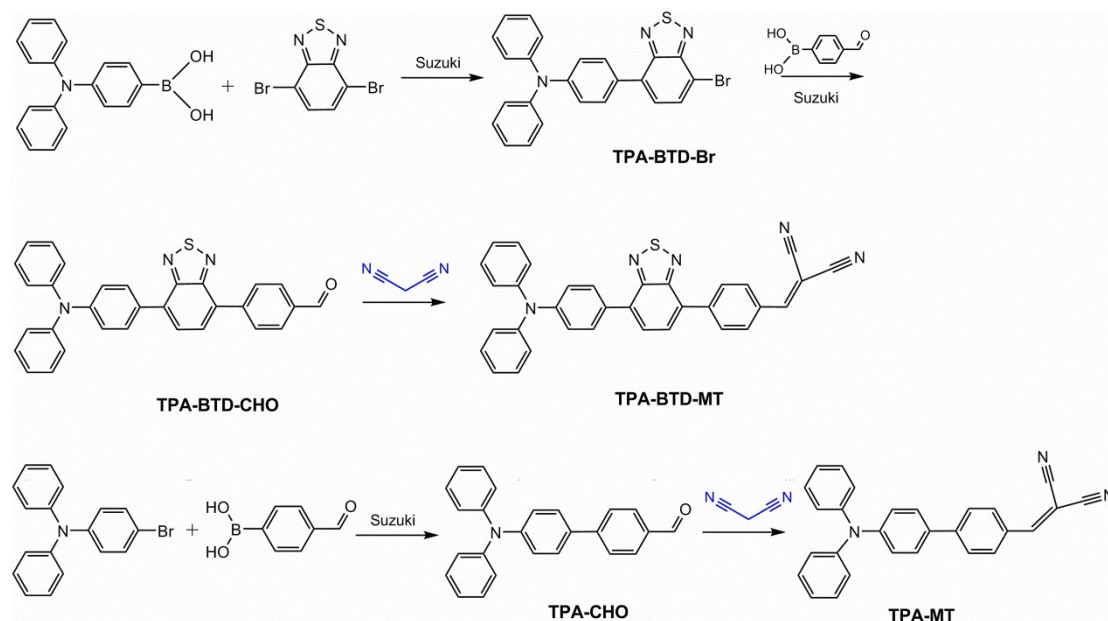
The prepared process for TPA-CHO was similar to that for TPA-BTD-CHO, except that compound 4-bromo-N,N-diphenylaniline (969 mg, 3.0 mol) was used instead of TPA-BTD-Br. The crude product was purified by column chromatography using DCM as an eluent to obtain target compound: (700 mg, 67% yield). <sup>1</sup>H NMR (CDCl<sub>3</sub>, 400 MHz, δ/ppm): 10.11 (s, 1H), 8.17 (d, *J* = 8.24 Hz, 2H), 8.05 (d, *J* = 8.44 Hz, 2H), 7.85-7.91 (m, 3H), 7.79 (d, *J* = 7.40 Hz, 1H), 7.19-7.32 (m, 8H), 7.06-7.10 (m, 2H). <sup>13</sup>C NMR (CDCl<sub>3</sub>, 100 MHz, δ/ppm): 191.88, 154.07, 153.91, 148.43, 147.38, 143.47, 135.76, 134.17, 130.95, 130.35, 130.05, 129.98, 129.79, 129.42, 129.05, 127.02, 125.08, 123.52, 122.64.

## 2.4. Synthesis of 2-(4-(7-(4-(diphenylamino)phenyl)benzo[c][1,2,5]thiadiazol-4-yl)benzylidene)malononitrile (TPA-BTD-MT)

A mixture of TPA-BTD-CHO (1.51 g, 3.1 mmol), malononitrile (2.52 g, 380 mmol) and ammonium acetate (4.78 g, 620 mmol) was added to acetic acid (200 mL). The reaction mixture was stirred at 120 °C for 8 h under argon. After being cooled to room temperature, the mixture was poured into water and extracted with DCM. The combined organic layer was dried over Na<sub>2</sub>SO<sub>4</sub> overnight and the organic phase was concentrated under reduced pressure to yield the product. The residue was purified by column chromatography using petroleum ether/DCM (v/v=1:1) as an eluent to give pure TPA-BTD-MT (1.48 g, 90% yield). <sup>1</sup>H NMR/ppm: 8.20 (d, *J* = 8.40 Hz, 2H), 8.07 (d, *J* = 8.48 Hz, 2H), 7.86-7.90 (m, 3H), 7.78-7.82 (m, 2H), 7.28-7.32 (m, 4H), 7.18-7.22 (m, 6H), 7.06-7.12 (m, 2H). <sup>13</sup>C NMR/ppm: 176.81, 159.06, 158.07, 154.09, 153.74, 148.58, 147.32, 143.64, 134.68, 131.51, 131.09, 130.41, 130.11, 129.98, 129.46, 129.20, 128.28, 126.93, 125.93, 125.15, 123.63, 122.50, 113.91, 112.79.

#### 2.5. Synthesis of 2-((4'-(diphenylamino)biphenyl-4-yl)methylene)malononitrile (TPA-MT)

The prepared process for TPA-MT was similar to that for TPA-BTD-MT, except that compound TPA-CHO (1.50 g, 4.3 mmol) was used instead of TPA-BTD-CHO. The crude product was purified by column chromatography using petroleum ether/DCM (v/v=1:1) as an eluent to obtain the target compound: (1.55 g, 91% yield). <sup>1</sup>H NMR/ppm: 7.96 (d, *J* = 8.28 Hz, 2H), 7.71-7.38 (m, 3H), 7.52 (d, *J* = 8.56 Hz, 2H), 7.25-7.32 (m, 4H), 7.07-7.16 (m, 8H). <sup>13</sup>C NMR/ppm: 159.09, 149.02, 147.13, 146.84, 131.57, 131.54, 129.50, 129.17, 127.95, 127.09, 125.17, 123.83, 122.67, 114.15, 113.05.



**Scheme S1.** Synthetic routes of TPA-BTD-MT and TPA-MT.

### 3. Solvatochromic Study

To determine the solvatochromic behavior of TPA-BTD-MT, its absorption spectra were recorded in different solvents with various polarities. Fig. S1A and B respectively demonstrate significant solvent dependent shifts in the maximum absorption band ( $\lambda_{Abs}$ ) and emission maxima ( $\lambda_{em}$ ). In different polarities of Hexane, Tetrachloromethane, Tetrahydrofuran (THF), Chloroform, and N,N-Dimethylformamide (DMF), Dimethyl sulfoxide (DMSO), and Acetonitrile, obvious shifts in  $\lambda_{em}$  of the probe were observed. Table S1 summarizes the absorption maxima, emission maxima, and Stokes shift of TPA-BTD-MT in the different solvents. Stokes shift ( $\Delta\nu$ ) was calculated as the difference ( $\Delta\nu = \nu_A - \nu_B$ ) between absorption and emission maxima obtained from the corrected spectra on the wavenumber scale.<sup>S1</sup> According to previous reports,<sup>S2-S4</sup> the results are mainly ascribed to the solvent relaxation process, which is a strong dipole–dipole interaction between the fluorophore in its excited state and the surrounding solvent molecules.<sup>S4, S5</sup>

The Lippert-Mataga equation (eq 1) was employed to investigate the solvent

relaxation process of the intramolecular charge transfer (ICT) fluorophore. In which  $C$  is a constant,  $\mu_e$  and  $\mu_g$  are the dipole moments in the excited state and ground state, respectively,  $\Delta\nu$  is the Stokes shift,  $\Delta f$  is the solvent polarity and is given by eq 2,  $\varepsilon$  is the dielectric constant and  $n$  is the optical refractive constant,  $h$  is Planck's constant,  $c$  is the speed of light, and  $a$  is the cavity radius of Onsagar's reaction field.

$$\Delta\nu = \nu_A - \nu_F = \frac{2\Delta f}{hca^3} (\mu_e - \mu_g)^2 + C \quad (1)$$

$$\Delta f = \frac{\varepsilon - 1}{2\varepsilon + 1} - \frac{n^2 - 1}{2n^2 + 1} \quad (2)$$

Fig. S1 and Table S1 show the linear relationship of Stoke shifts of TPA-BTD-MT with the changes of  $\Delta f$ . A positive slope ( $R=0.9673$ ) was obtained, which suggests that TPA-BTD-MT shows general solvent effect. According to the previous reports, the gross solvent polarity indicator scale such as  $E_T30$  is more applicable.<sup>S1,56</sup> As shown in Fig. S1D, Stokes shift increased linearly with increasing  $E_T30$  values ( $R=0.9443$ ).<sup>S6</sup> These results indicate that the emission of the TPA-BTD-MT comes from the highly polarized excited states induced by the ICT transition. Therefore, the results further prove that the fluorescence change of the TPA-BTD-MT probe toward  $CN^-$  is based on the ICT process.

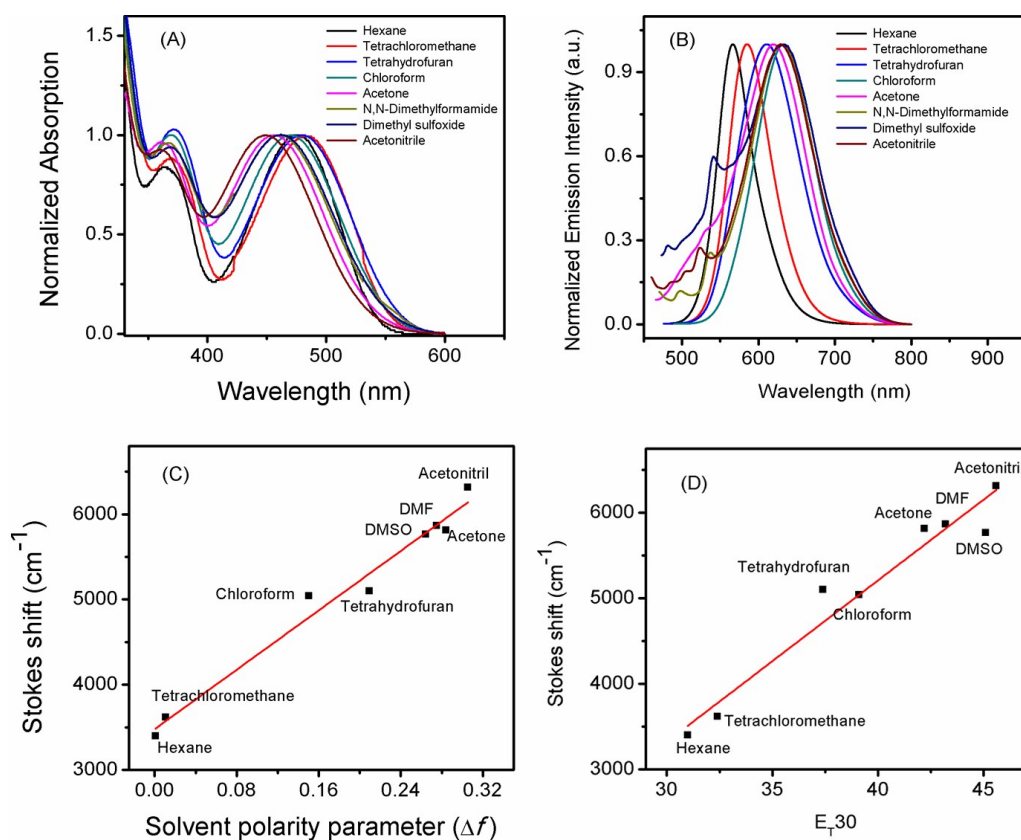


**Fig. S1.** Normalized absorption (A) and emission spectral changes (B) of TPA-BTD-MT in different polarities of solvents. (C) Lippert–Mataga plot for the variation of Stokes shift as a function of orientation polarizability of the solvents. (D) Correlation of solvent induced Stokes shift of TPA-BTD-MT with  $E_T30$  parameter.

**Table S1** The relevant parameters of TPA-BTD-MT in solvatochromic study with various solvents.

Solvents	$\epsilon$	$n$	$\lambda_{abs}/nm$	$\lambda_{em}/nm$	$\Delta\nu/cm^{-1}$	$\Delta f$	$E_T30^{56}$
Hexane	1.89	1.37226	475	566.4	3397.26	0.00091	31.0
Tetrachloromethane	2.238	1.46044	483	585.2	3615.76	0.01094	32.4
Tetrahydrofuran	7.58	1.4073	466	611.2	5097.97	0.20954	37.4
Chloroform	4.9	1.4467	480	633.2	5040.53	0.15036	39.1
Acetone	20.7	1.359	456	620.4	5811.19	0.28420	42.2
N,N-Dimethylformamide	36.71	1.42817	460	630	5866.11	0.27516	43.2
Dimethyl sulfoxide	48.9	1.4773	463	631.6	5765.47	0.26442	45.1
Acetonitrile	37.5	1.34411	450	628.6	6313.85	0.30541	45.6

#### 4. Optical Characteristic Analysis

For optical characterization, the stock solution of the probe (1 mM) was prepared by dissolving TPA-MT or TPA-BTD-MT into tetrahydrofuran (THF). Ultraviolet–visible (UV–vis) absorption spectra and emission spectra were recorded on a TU-1901 model UV–vis spectrophotometer (Persee, China) and a RF-5301PC spectrophotometer (Shimadzu, Japan). To obtain the standard curves and the limit of detection (LOD) of the TPA-BTD-MT probe toward cyanide, fluorescence titration was carried out in THF solution, and calculated using the equation of  $DL = 3\sigma/S$ , where  $\sigma$  is the standard deviation of blank measurements and  $S$  is the slope of the standard curve between fluorescence intensity and sample concentration.

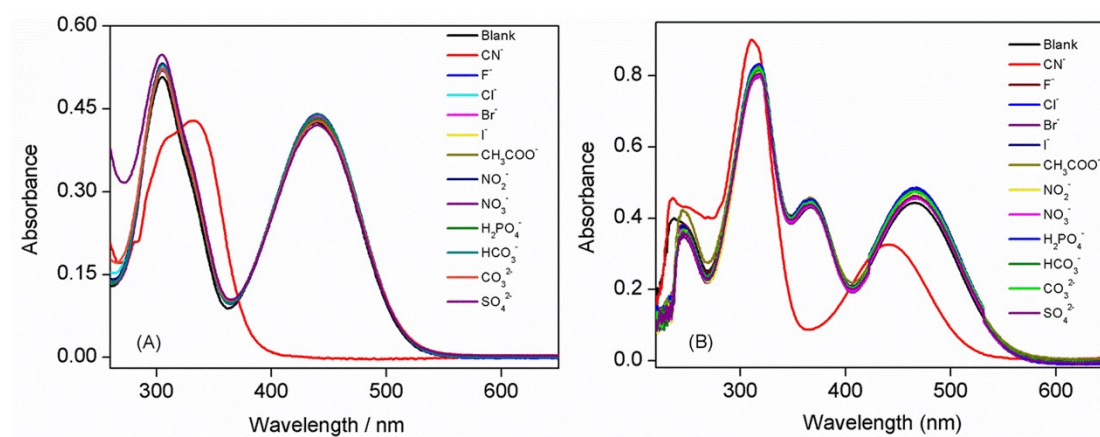


**Fig. S2.** UV–vis absorption spectra of 20  $\mu\text{M}$  TPA-MT (A) and TPA-BTD-MT (B) with 2.0 equivalents of different anions ( $\text{CN}^-$ ,  $\text{F}^-$ ,  $\text{Cl}^-$ ,  $\text{Br}^-$ ,  $\text{I}^-$ ,  $\text{CH}_3\text{COO}^-$ ,  $\text{NO}_2^-$ ,  $\text{NO}_3^-$ ,  $\text{H}_2\text{PO}_4^-$ ,  $\text{HCO}_3^-$ ,  $\text{CO}_3^{2-}$ , and  $\text{SO}_4^{2-}$ ) in THF.



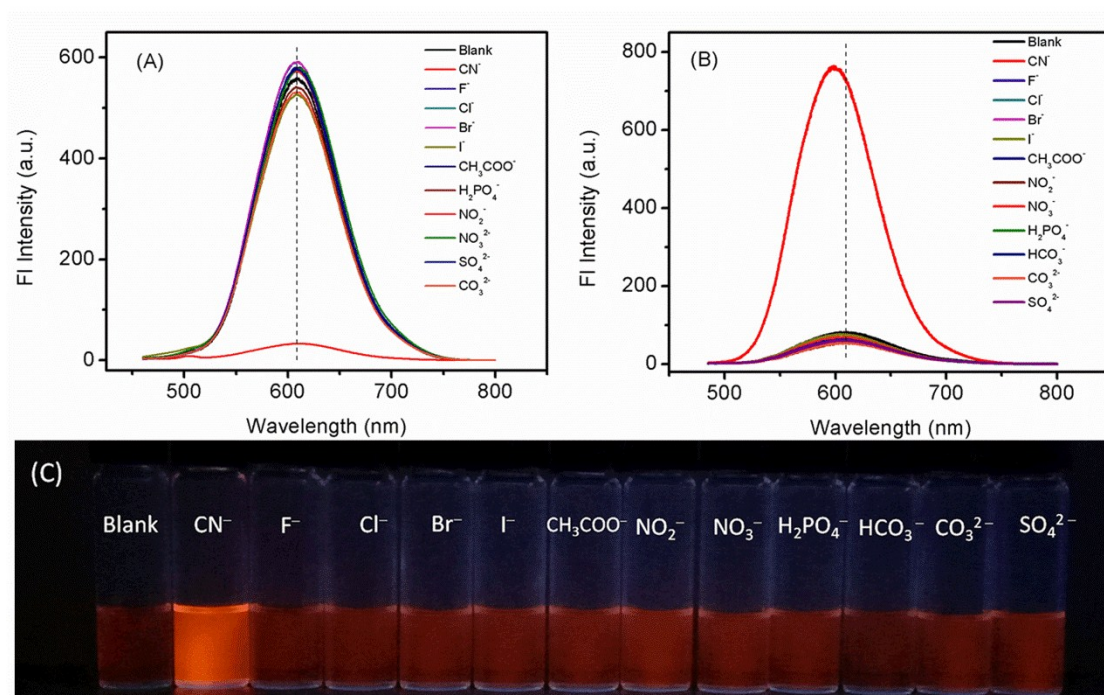


**Fig. S3.** Fluorescence spectra of 20  $\mu\text{M}$  TPA-MT (A) and TPA-BTD-MT (B) upon addition of 2 equivalents of different anions ( $\text{CN}^-$ ,  $\text{F}^-$ ,  $\text{Cl}^-$ ,  $\text{Br}^-$ ,  $\text{I}^-$ ,  $\text{CH}_3\text{COO}^-$ ,  $\text{NO}_2^-$ ,  $\text{NO}_3^-$ ,  $\text{H}_2\text{PO}_4^-$ ,  $\text{HCO}_3^-$ ,  $\text{CO}_3^{2-}$ , and  $\text{SO}_4^{2-}$ ) in THF and corresponding photographs (C).

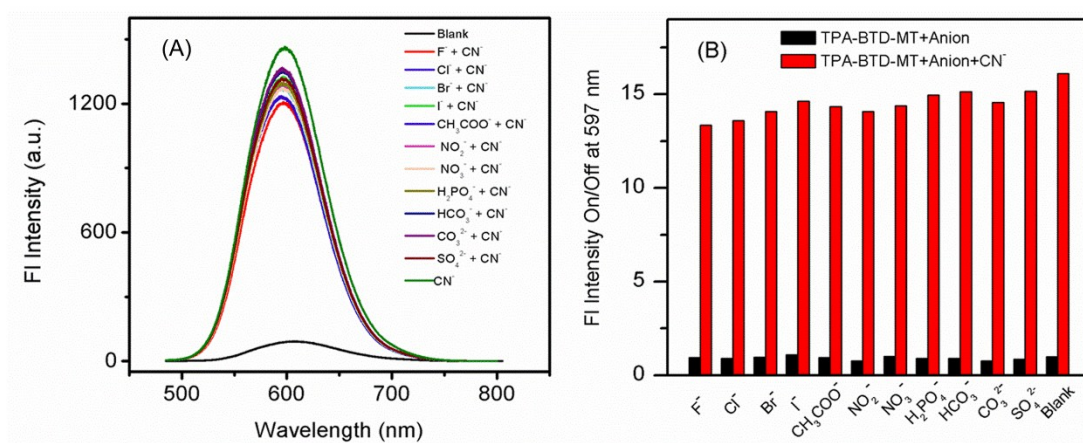


**Fig. S4.** (A) Fluorescence spectra of 20  $\mu\text{M}$  TPA-BTD-MT with 4.0 equivalents of  $\text{CN}^-$  upon addition of different anions (4.0 equivalents) in THF; (B) Fluorescence intensity On/Off at 596 nm with TPA-BTD-MT intensity (blank solution) as reference.

## 5. Computations and the sensing mechanism of the TPA-BTD-MT probe to $\text{CN}^-$

The molecular structure of compounds TPA-MT, TPA-BTD-MT, TPA-MT-CN, and TPA-BTD-MT-CN was analyzed by the Gaussian 09 program with density functional theory (DFT) at the B3LYP/6-31G\* level.<sup>57,58</sup> The location of the highest occupied molecular orbitals (HOMOs), the lowest unoccupied molecular orbitals (LUMOs), and the electronic properties of TPA-MT, TPA-BTD-MT, TPA-MT-CN, and TPA-BTD-MT-CN were studied using the B3LYP/6-31G\* method in water solvent. To gain insight into the electronic properties of TPA-MT, TPA-BTD-MT, TPA-MT-CN, and TPA-BTD-MT-CN, time-dependent density functional theory (TD-DFT) calculations were used on ground state geometries and the electronic absorption spectra at the B3LYP/6-31G\*\* level. The PCM model was used in water solvent.

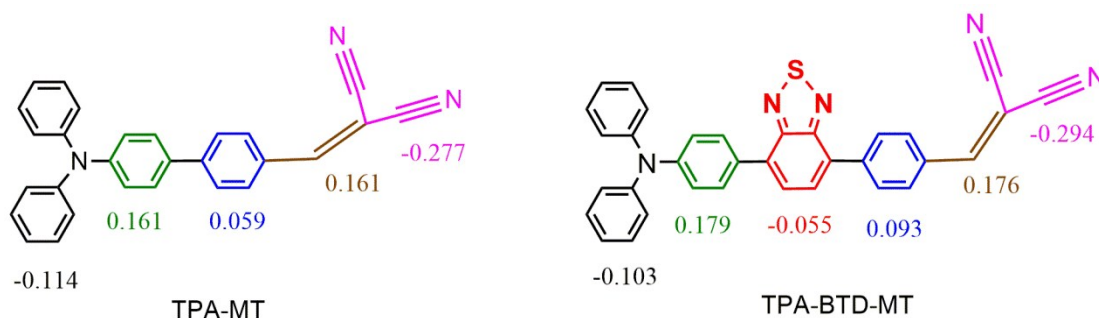


**Fig. S5.** Calculated partial charges on different units in TPA-MT and TPA-BTD-MT.

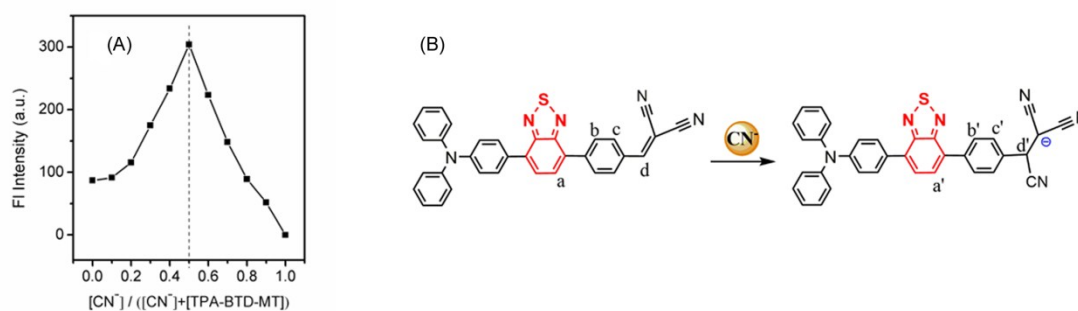


**Fig. S6.** (A) Job plots for the interaction between TPA-BTD-MT and  $\text{CN}^-$ . (B) Suggested mechanism for the reaction.

## 6. Kinetic study

The kinetic processes of the interaction between TPA-BTD-MT and  $\text{CN}^-$  had

been performed with various concentration of  $\text{CN}^-$ . Fig. S7A shows the time-dependent change in fluorescence spectra of 20.0  $\mu\text{M}$  TPA-BTD-MT obtained after addition of 2 equivalents  $\text{CN}^-$  (The spectra with other equivalents were not supplied due to the similar change to that of 2 equivalents). After adding  $\text{CN}^-$ , the fluorescence intensity of the TPA-BTD-MT probe increased and reached the plateau region in less than 10 min, and remained stable. As plotted in Fig. S7B, the change in the emission intensity of the TPA-BTD-MT probe with various equivalents shows similar results, suggesting that the binding process might be completed within 10 min.

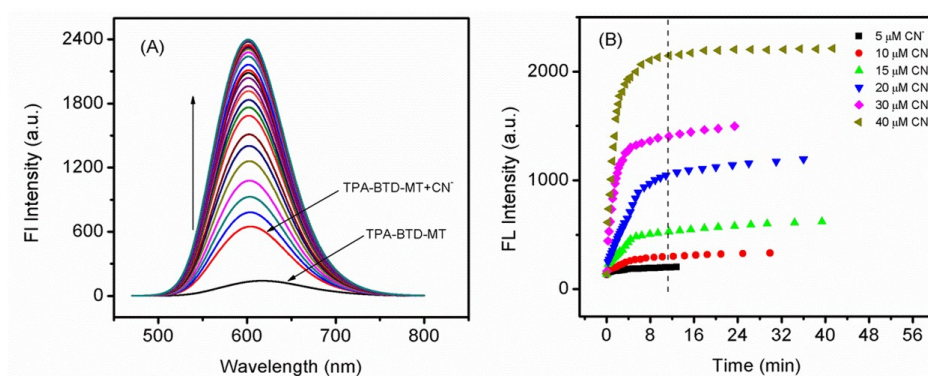


**Fig. S7** (A) Time-dependent changes in the fluorescence spectra of 20.0  $\mu\text{M}$  TPA-BTD-MT measured after addition of 2.0 equivalents of  $\text{CN}^-$  (40.0  $\mu\text{M}$ ) in THF ( $\lambda_{\text{ex}}=438$ ). (B) Time-dependent changes fluorescence intensity of TPA-BTD-MT at the maximum emission ( $\lambda_{\text{em}}$ ) with different equivalents of  $\text{CN}^-$ .

## 7. Study on solubility

Before cytotoxicity test, the solubility of the TPA-BTD-MT probe in aqueous media was studied. Firstly, 10 mM TPA-BTD-MT probe in DMSO was prepared. Various volumes of 10 mM TPA-BTD-MT were added to 2.00 mL pure water. In the presence of DMSO, TPA-BTD-MT was well dissolved in water/DMSO mixed solution (Fig. S8A). The concentration of TPA-BTD-MT can be higher than 300  $\mu\text{M}$  in

water/DMSO (V/V: 33/1) without precipitate.

However, we used 3.0 mL pure water to dissolve 0.58 mg TPA-BTD-MT, which could not be dissolved in the absence of DMSO (Fig. S8B). Then, we gradually added DMSO into the water, TPA-BTD-MT still could not be dissolved well (Fig. S8C). In another group, we first used 200  $\mu$ L DMSO to dissolve 0.54 mg TPA-BTD-MT, and then, 3.0 mL and even more volume of water was added, the mixed solution was homogeneous and stable (Fig. S8D). Therefore, in the presence of DMSO, TPA-BTD-MT can be dissolved well in water and used to perform the experiments in biological system.

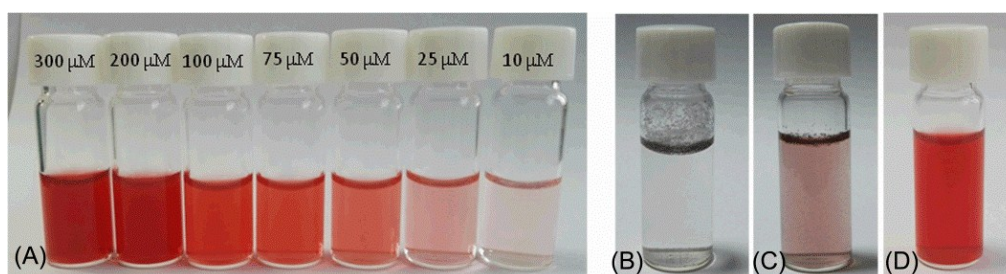


**Fig. S8** (A) Color change of 3.00 mL water with addition of various volume of 10.0 mM TPA-BTD-MT (From right to left: 2.00, 5.00, 10.00, 15.00, 20.00, 40.00, and 60.00  $\mu$ L; and the concentration is 10.0, 25.0, 50.0, 75.0, 100.0, 200.0, 300.0  $\mu$ M, respectively). The picture of 0.58 mg TPA-BTD-MT dispersed in 3.0 mL pure water without DMSO (B), and 300  $\mu$ L DMSO was further added alone (C). (D) 0.54 mg TPA-BTD-MT was first dissolved in 200  $\mu$ L DMSO and 3.0 mL pure water was then added.

## 8. Cell Cytotoxicity Assays

Beas-2B cells were purchased from Cobioer Biosciences Co., LTD (Nanjing, China). The Beas-2B cells were grown in Dulbecco's modified Eagle's medium (DMEM) supplemented with 10% fetal bovine serum at 37  $^{\circ}$ C in a humidified environment of 5% CO<sub>2</sub>. First,  $1 \times 10^4$  BEAS-2B cells/well in 96-well plates were grown in cell culture medium for 10 h and were then washed twice with 0.01 M PBS. The complete cell culture medium was replaced by cell culture medium containing the required



concentration of tetrabutylammonium cyanide ((TBA)CN), TPA-BTD-MT, or their complex. After incubation for 24 h, the viability of cells was assessed by the MTT assay.

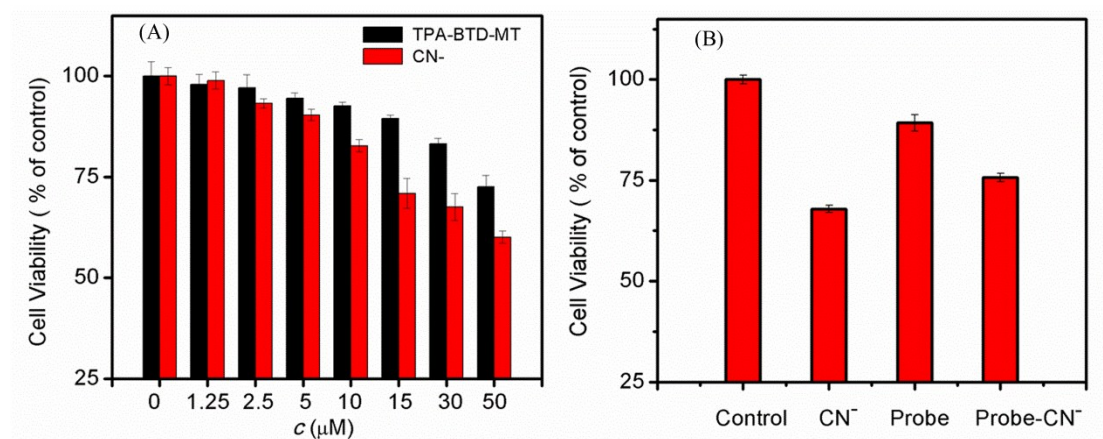


**Fig. S9.** (A) Cell viability of BEAS-2B in cell culture medium with various concentrations of TPA-BTD-MT and CN<sup>-</sup>; (B) Cell viability of BEAS-2B in cell-culture medium with 0 or 15 μM CN<sup>-</sup>, 15 μM TPA-BTD-MT (expressed as probe in figure), and the mixture of 15 μM TPA-BTD-MT and CN<sup>-</sup> as measured by MTT assay (A high concentration of CN<sup>-</sup> was first prepared in DMSO and it was then diluted to the required concentration using cell culture medium, which was then used to replace the cell-culture medium for cytotoxicity experiments).

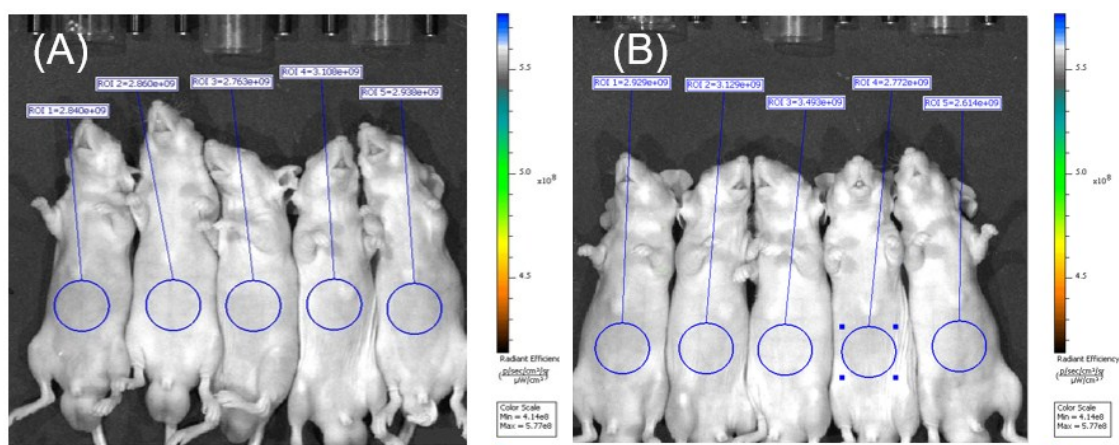
## 9. Bioimaging Application in Living Cells

The stock solution of 1 mM TPA-BTD-MT probe was prepared in dimethyl sulfoxide (DMSO) for use. Beas-2B cells were pretransferred to a culture chamber cover slide and then incubated for 10 h. After being rinsed with 0.01 M PBS, the cells were treated with DMEM medium, CN<sup>-</sup> (5 μM), and TPA-BTD-MT (10 μM) and were then incubated for 60 min at 37°C. Another group of cells with TPA-BTD-MT (10 μM) was first incubated at 37 °C for 30 min and then 5 μM cyanide was added and followed by incubation for another 30 min. After that, the culture medium was removed and the treated cells were rinsed with 0.01 M PBS 3 times before

observation. All of the cell images were performed on a laser confocal scanning microscope (Leica, TCS sp5II); the excitation wavelength for live cell imaging was 485 nm.

## 10. Bioimaging Application in Living mice

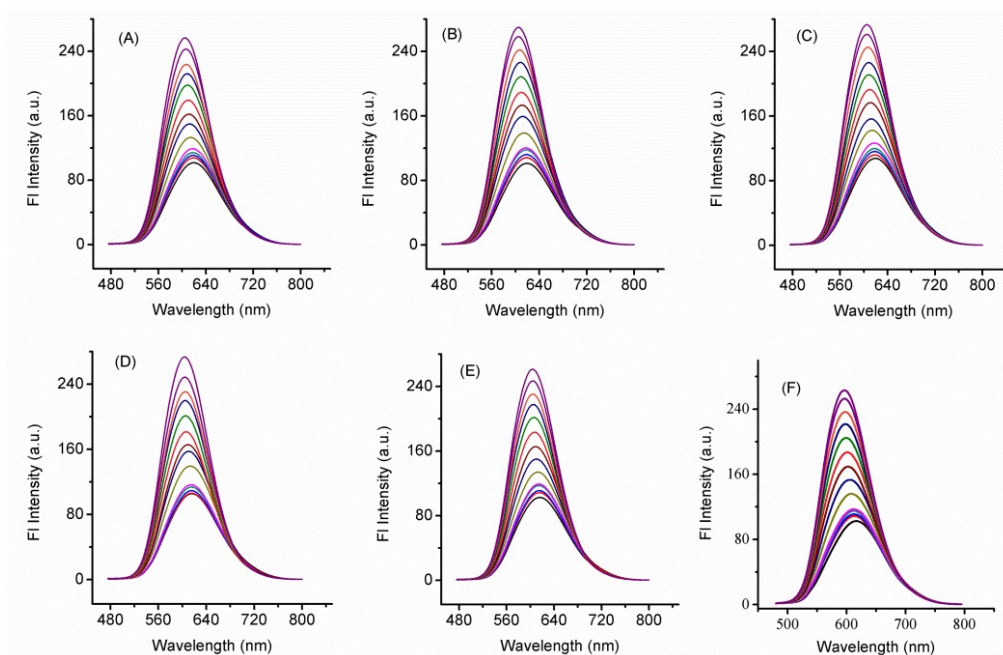
Six-week-old BALB/C mice were anesthetized via the intraperitoneal injection of 1% pentobarbitalum natricum solution (75 mg/kg). Then one group (five mice) was used as control and other two groups were given an intraperitoneal injection of 100  $\mu$ L 2.5 mM  $\text{CN}^-$  and 50  $\mu$ L 10 mM TPA-BTD-MT, respectively. After 10 min, the mice were imaged by Lumina XRMS series III system. The fourth group was first injected 100  $\mu$ L 2.5 mM  $\text{CN}^-$  ( $\text{H}_2\text{O}/\text{DMSO}$ ), after 10 min, which was then injected 50  $\mu$ L 10 mM TPA-BTD-MT (DMSO) at the same point followed by imaging in the same conditions 10 min later. The animal experiments were performed by the Hibio Tech Co., Ltd (Hangzhou, China) and were treated with standard procedure.



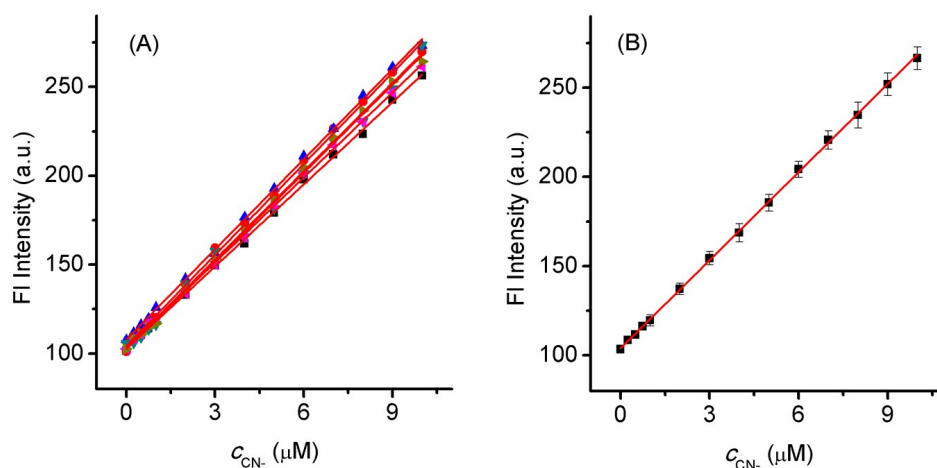
**Fig. S10.** In vivo fluorescence imaging of BALB/C living mice without  $\text{CN}^-$  (A) and injected with 0.25  $\mu\text{mol}$   $\text{CN}^-$  (100  $\mu\text{L}$  2.5 mM  $\text{CN}^-$  in  $\text{H}_2\text{O}/\text{DMSO}$  solution) (B)

## 11. The determination of the TMP-BTD-MT probe toward $\text{CN}^-$

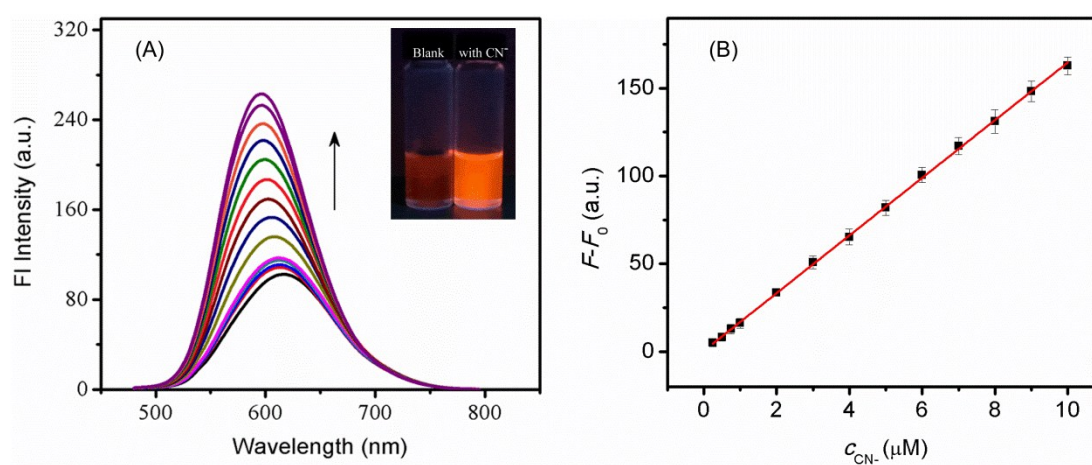
To obtain the standard curve for  $\text{CN}^-$  determination, we repeated the experiments for six groups (Fig. S11A–F). Standard curve for every group and standard curve with average values were obtained (Fig. S12). To improve the accuracy for the standard curve, we used the difference ( $\Delta F = F - F_0$ ) between the fluorescence of the TPA-BTD-MT probe ( $F_0$ ) and the probe with  $\text{CN}^-$  system ( $F$ ) as signal (Y-axis) to fit the standard curve. The equation of standard curve was  $\Delta F = 0.4437c + 16.43$  ( $R=0.9992$ ) and the linear concentration range was  $0.025\text{--}10.0\ \mu\text{M}$  (Fig. S13). The limit of detection was  $0.087\ \mu\text{M}$  calculated with  $3\sigma/S$ . With the standard curve, the determined results for the real food samples were supplied in Table S3. Good recoveries between 97.18% and 101.73% and repeatability of the presented method suggested the analysis based on the proposed TMP-BTD-MT probe is reliable for  $\text{CN}^-$  sensing in food analysis.



**Fig. S11** (A–E) Fluorescence spectra of the TPA-BTD-MT probe ( $10.0\ \mu\text{M}$ ) in THF upon addition of various concentrations of  $\text{CN}^-$  standard aqueous solution for five other groups, (F) The original figure in Supporting Information of the manuscript at the same experimental conditions with A–E.



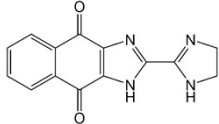
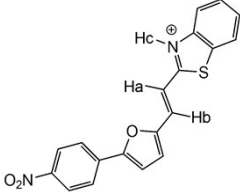
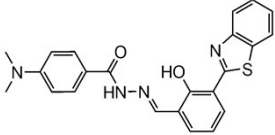
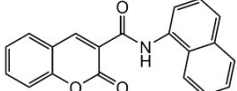
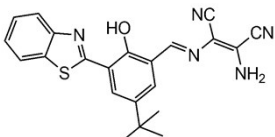
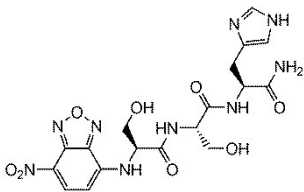
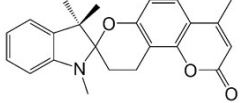
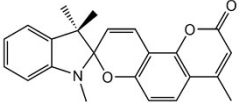
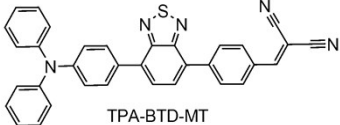
**Fig. S12** (A) The plots of fluorescence intensity (obtained from Fig. S3) vs. the concentration of  $C_{CN^-}$  for six repeated experiments. (B) Plot between the average fluorescence intensity at the maximum emission wavelength and the concentration of  $C_{CN^-}$  in the range of 0–10.0  $\mu M$ . The error bars represent standard deviation of the six independent measurements ( $n=6$ ).



**Fig. S13.** (A) Fluorescence spectra of the TPA-BTD-MT probe (10.0  $\mu M$ ) in THF upon addition of various concentrations of  $C_{CN^-}$  standard aqueous solution; (B) The plots of fluorescence intensity vs. the concentration of  $C_{CN^-}$ . (B) Plot between  $\Delta F (= F-F_0)$  and the concentration of  $C_{CN^-}$  in the range of 0.025–10.0  $\mu M$ . The error bars represent standard deviation of the six independent measurements ( $n=6$ ).



**Table S2.** Comparison of the TPA-BTD-MT probe with the reported fluorescent sensor for the detection of  $\text{CN}^-$ .

Structure of probes	Sensor type	Solvent	LOD ( $\mu\text{M}$ )	Reference
	Turn-off	DMSO/ $\text{H}_2\text{O}$ (1:1, v/v)	1	S9
	Turn-off	DMSO/ $\text{H}_2\text{O}$ (1:1, v/v)	0.11	S10
	Turn-on	DMF/ $\text{H}_2\text{O}$ (1:9, v/v)	0.15	S11
	Turn-on	DMSO/ $\text{H}_2\text{O}$ (8:2, v/v)	0.115	S12
	Turn-on	DMF/ $\text{H}_2\text{O}$ (1:1, v/v)	0.16	S13
	Turn-on	Aqueous solution	0.0249	S14
	Turn-on	Aqueous solution	1	S15
	Turn-on	$\text{H}_2\text{O}$ /MeCN (7/3, v/v)	0.4	S16
 TPA-BTD-MT	Turn-on	THF	0.087	This work

**Table S3.** The detected results of CN<sup>-</sup> in real samples with TPA-BTD-MT probe

<b>Sample</b>	<b>Detected (<math>\mu\text{M}</math>)</b>	<b>Added (<math>\mu\text{M}</math>)</b>	<b>Found (<math>\mu\text{M}</math>)</b>	<b>Recovery (%)</b>	<b>Relative error (%)</b>
Sprouting potato	1.698	4.0	5.597	97.48	2.53
	1.898	4.0	5.834	98.40	1.60
	1.807	4.0	5.792	99.63	0.38
Bitter seeds	0.803	4.0	4.690	97.18	2.83
	0.663	4.0	4.647	99.60	0.40
	0.615	4.0	4.617	100.05	0.05
Apple seeds	0.158	4.0	4.142	99.60	0.4
	0.358	4.0	4.313	98.88	1.13
	0.182	4.0	4.069	97.18	2.83
Cassava	0.925	4.0	4.891	99.15	0.85
	0.979	4.0	5.025	101.15	1.15
	0.913	4.0	4.982	101.73	1.73

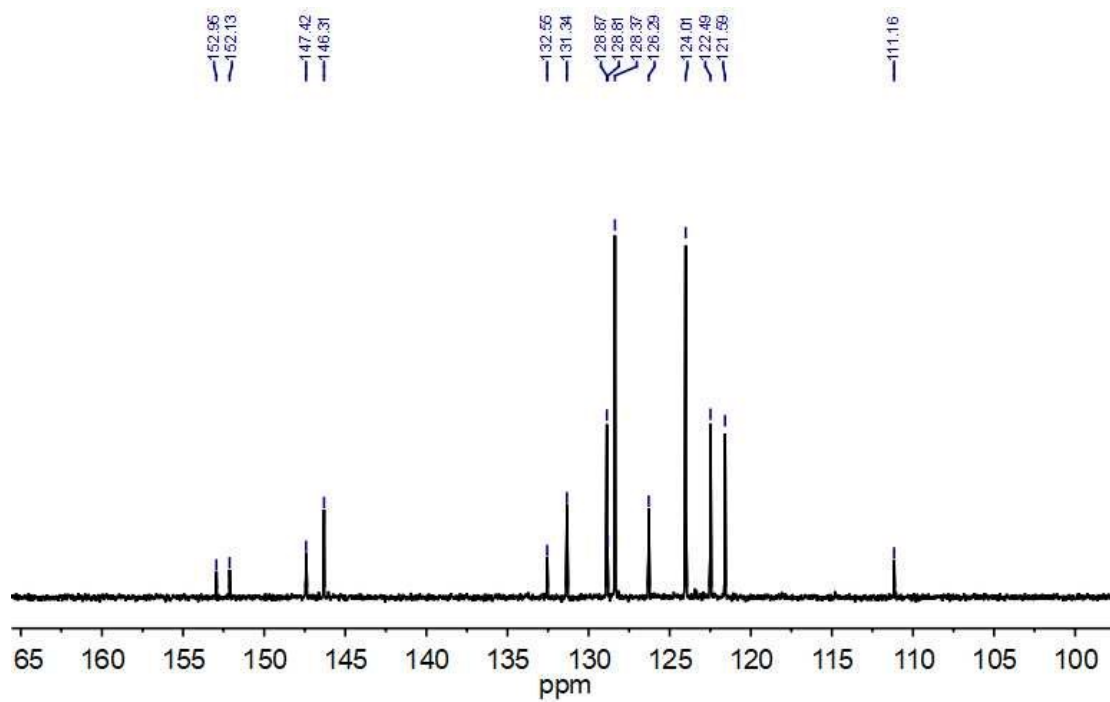
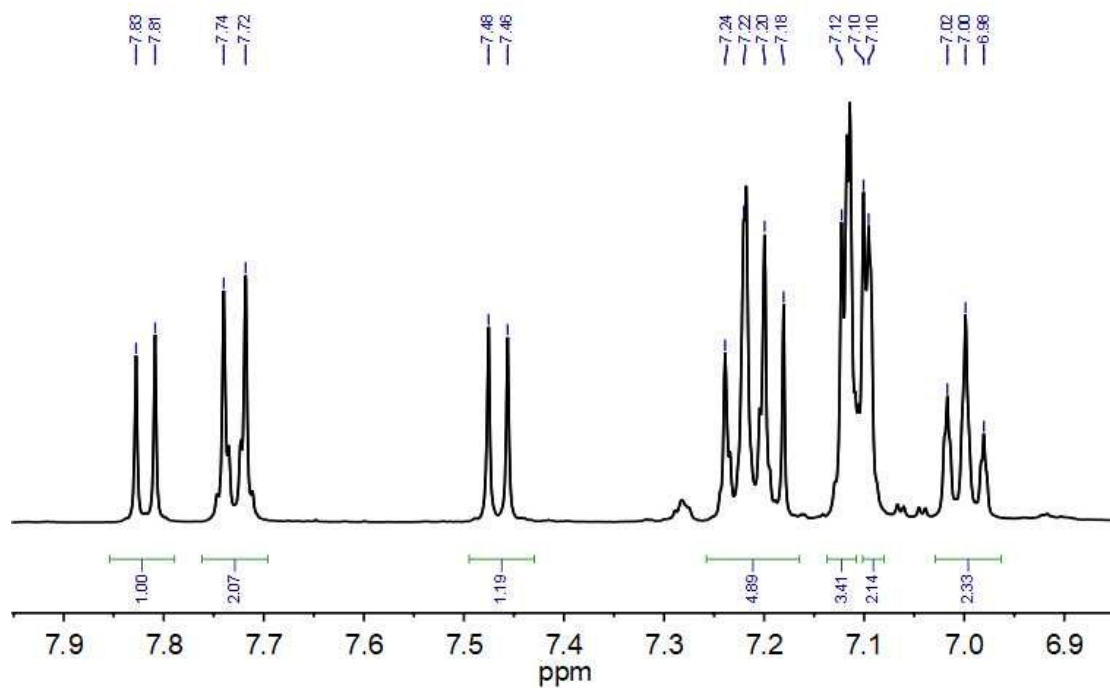


**Fig. S14.**  $^1\text{H}$  NMR and  $^{13}\text{C}$  NMR spectra of TPA-BTD-Br.

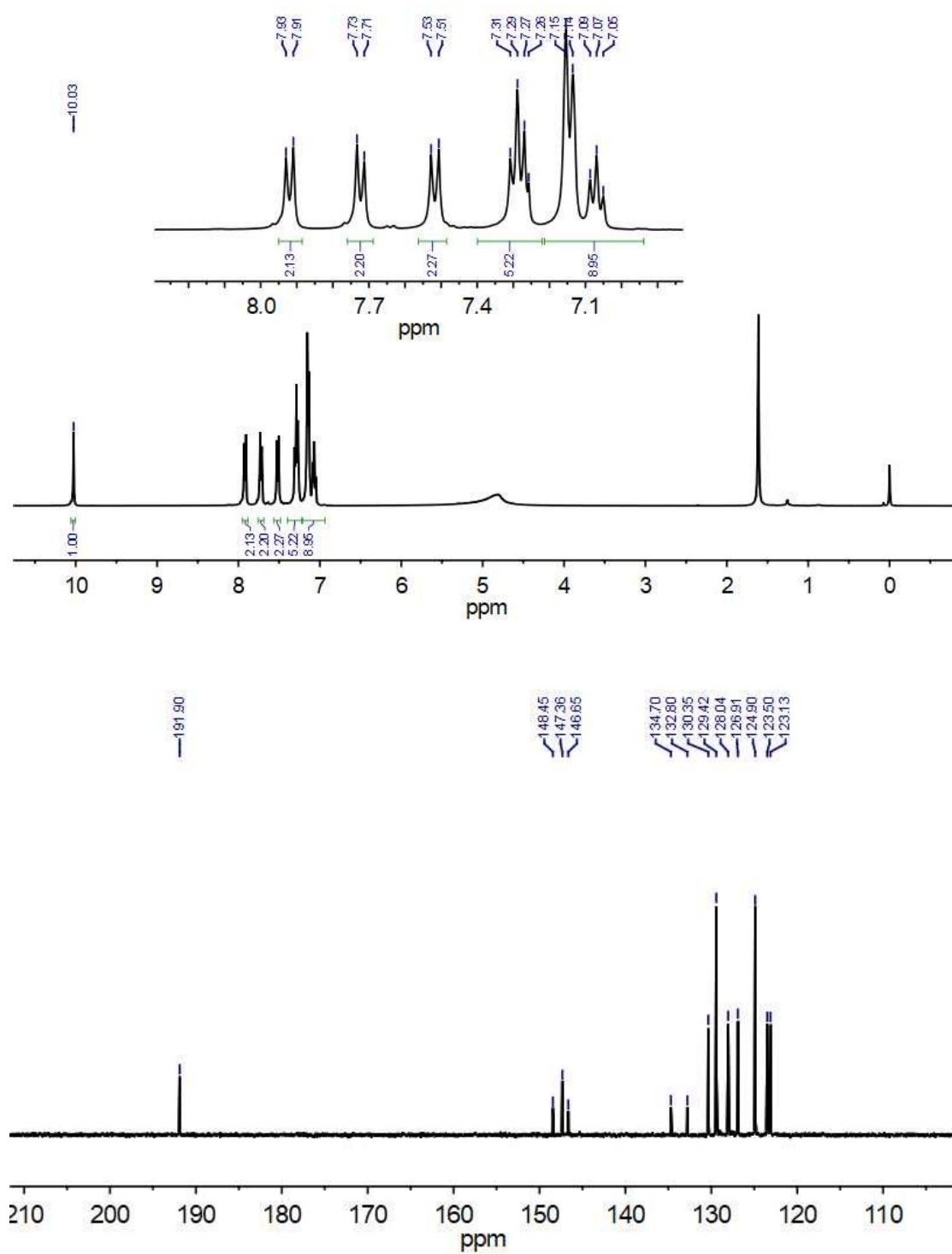


**Fig. S15.**  $^1\text{H}$  NMR and  $^{13}\text{C}$  NMR spectra TPA-BTD-CHO.

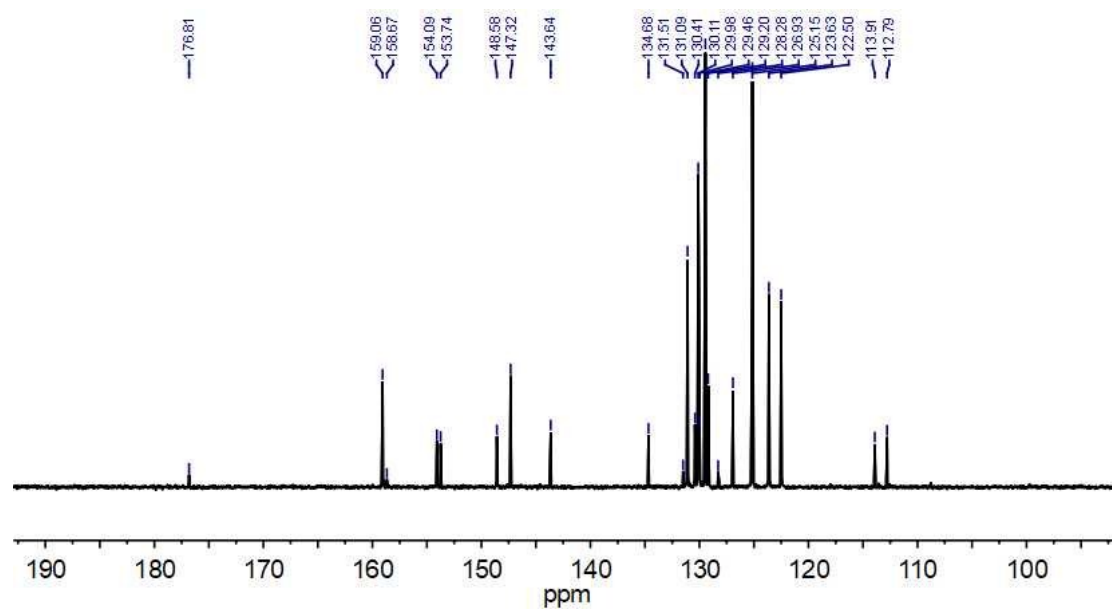
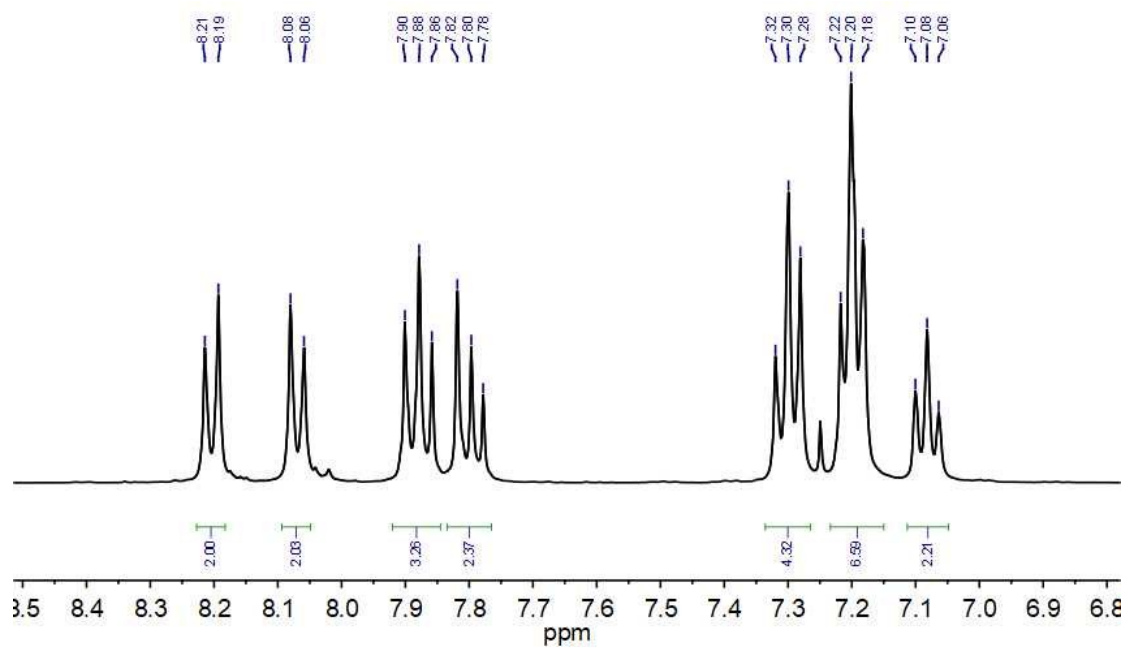


**Fig. S16.**  $^1\text{H}$  NMR and  $^{13}\text{C}$  NMR spectra of TPA-BTD-MT.

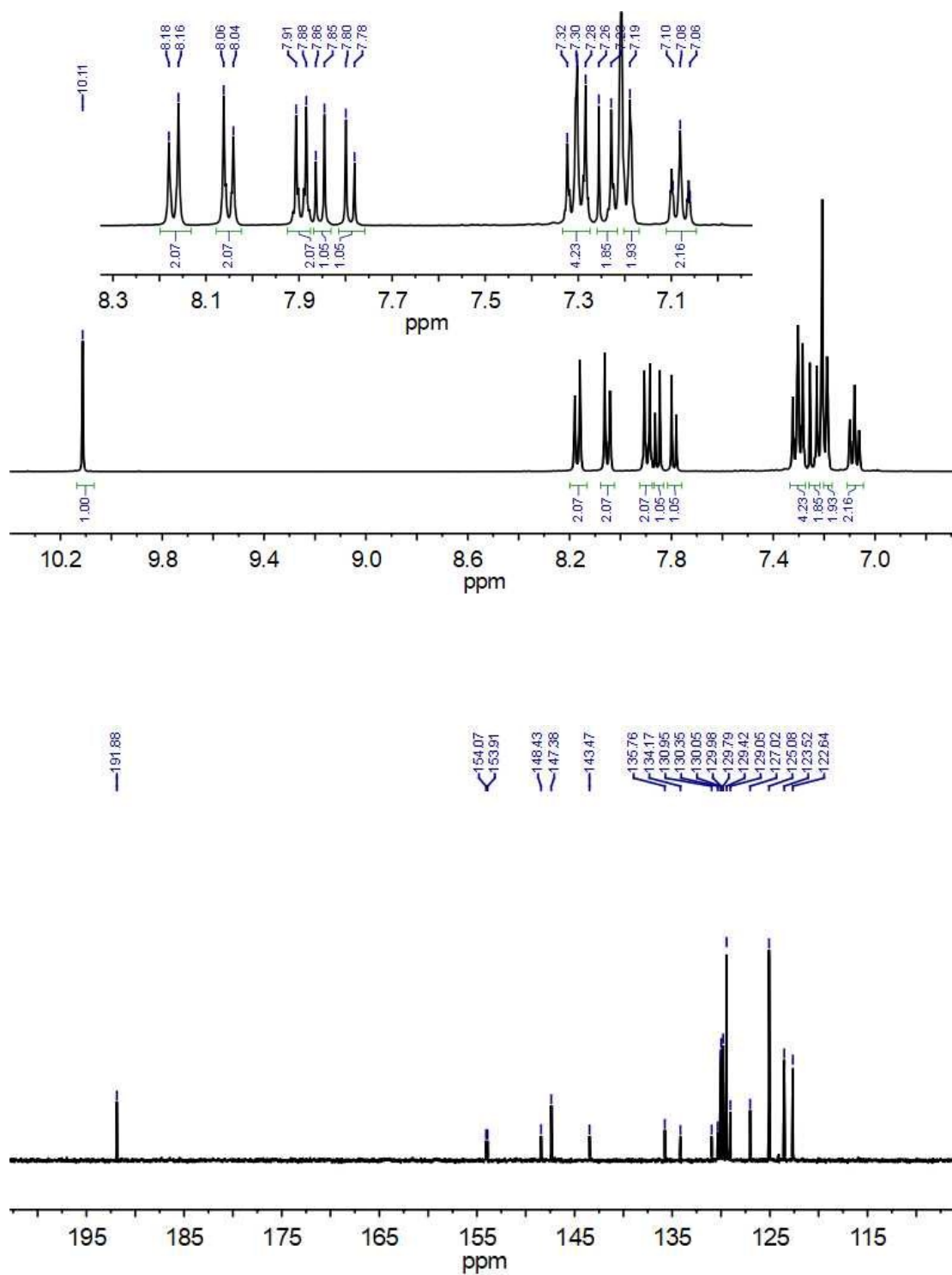
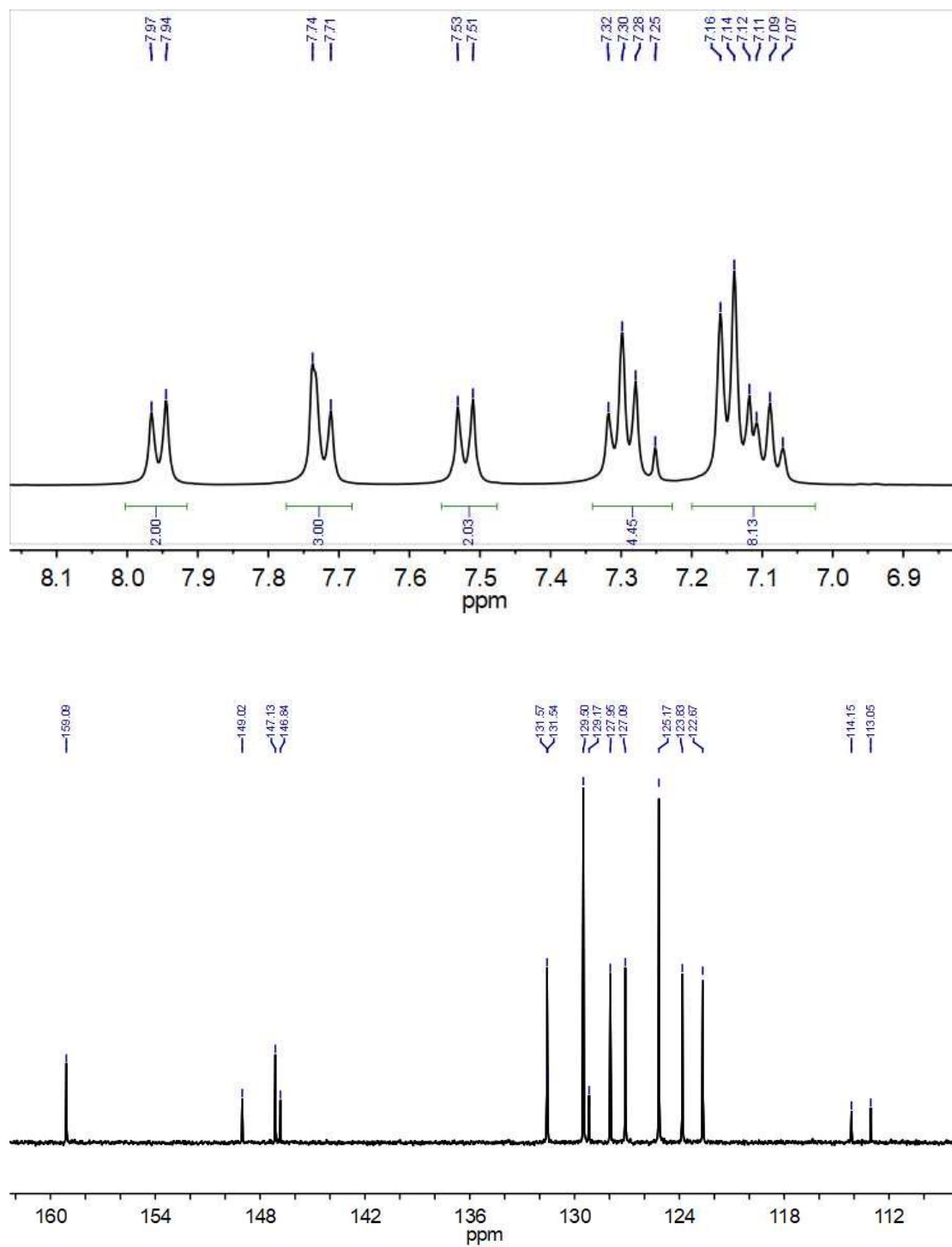


Fig. S17.  $^1\text{H}$  NMR and  $^{13}\text{C}$  NMR spectra of TPA-CHO.



**Fig. S18.**  $^1\text{H}$  NMR and  $^{13}\text{C}$  NMR spectra of TPA-MT.

## References

- S1. D. Patra and C. Barakat, *Spectrochimica Acta Part A*, 2011, **79**, 1034–1041.
- S2. G. Fu, H. Zhang, Y. Yan and C. Zhao, *J. Org. Chem.*, 2012, **77**, 1983–1990.
- S3. P.G. Rao, B. Saritha and T. S. Rao, *J. Photoch. Photobio. A*, 2019, **372**, 177–185.
- S4. Y. Li, T. Ren and W.-J. Dong *J. Photoch. Photobio. A*, 2013, **251**, 1–9.
- S5. J. Herbich and A. Kapturkiewicz, *J. Am. Chem. Soc.*, 1998, **120**, 1014–1029.
- S6. C. Reichardt, *Chem. Rev.*, 1994, **94**, 2319–2358.
- S7. M.J. Frisch, G.W. Trucks, H.B. Schlegel, G.E. Scuseria, M.A. Robb, J.R. Cheeseman, G. Scalmani, V. Barone, B. Mennucci, G.A. Petersson, H. Nakatsuji, M. Caricato, X. Li, H.P. Hratchian, A.F. Izmaylov, J. Bloino, G. Zheng, J. L. Sonnenberg, M. Hada, M. Ehara, K. Toyota, R. Fukuda, J. Hasegawa, M. Ishida, T. Nakajima, Y. Honda, O. Kitao, H. Nakai, T. Vreven, J.A. Montgomery, J.E. Peralta, F. Ogliaro, M. Bearpark, J.J. Heyd, E. Brothers, K.N. Kudin, V.N. Staroverov, R. Kobayashi, J. Normand, K. Raghavachari, A. Rendell, J. C. Burant, S.S. Iyengar, J. Tomasi, M. Cossi, N. Rega, J.M. Millam, M. Klene, J.E. Knox, J.B. Cross, V. Bakken, C. Adamo, J. Jaramillo, R. Gomperts, R. E. Stratmann, O. Yazyev, A. J. Austin, R. Cammi, C. Pomelli, J.W. Ochterski, R. L. Martin, K. Morokuma, V.G. Zakrzewski, G.A. Voth, P. Salvador, J.J. Dannenberg, S. Dapprich, A.D. Daniels, O. Farkas, J.B. Foresman, J.V. Ortiz, J. Cioslowski, D.J. Fox, *Gaussian 09, Revision A.02*, Gaussian, Inc., Wallingford CT, 2009.
- S8. A.D. Becke, *J. Chem. Phys.*, 1993, **98**, 5648–5652.
- S9. P.R. Lakshmi, P. Jayasudha and K.P. Elango, *Spectrochim. Acta Part A*, 2019, **213**, 318–323.
- S10. Y. Wang, J. Wang and Q. Xian, *Talanta*, 2018, **190**, 487–491.
- S11. W. Xu, G. Han, P. Ma, Q. Diao, L. Xu, X. Liu, Y. Sun, X. Wang and D. Song, *Sens. Actuators B*, 2017, **251**, 366–373
- S12. J. Chen, W. Li, Q. Li, Q. Lin, H. Yao, Y. Zhang and T. Wei, *Chin. J. Chem.*, 2017, **35**, 1165–1169.
- S13. K. Keshav, P. Torawane, M.K. Kumawat, K. Tayade, S.K. Sahoo, R. Srivastava and A. Kuwar, *Biosens. Bioelectron.*, 2017, **92**, 95–100.



S14.K.H. Jung and K.-H. Lee, *Anal. Chem.*, 2015, **87**, 9308–9314.

S15.Y. Shiraishi, M. Nakamura, N. Hayashi and T. Hirai, *Anal. Chem.*, 2016, **88**, 6805–6811.

S16.Y. Shiraishi, M. Nakamura, K. Yamamoto and T. Hirai, *Chem. Commun.*, 2014, **50**, 11583–11586.